

The diagnostic performance of magnetic resonance spectroscopy in differentiating high-from low-grade gliomas: A systematic review and meta-analysis

Qun Wang¹ · Hui Zhang² · JiaShu Zhang¹ · Chen Wu¹ · WeiJie Zhu³ · FangYe Li¹ · XiaoLei Chen¹ · BaiNan Xu¹

Received: 14 July 2015 / Revised: 19 September 2015 / Accepted: 23 September 2015 / Published online: 15 October 2015
© European Society of Radiology 2015

Abstract

Objective Magnetic resonance spectroscopy (MRS) is a powerful tool for preoperative grading of gliomas. We performed a meta-analysis to evaluate the diagnostic performance of MRS in differentiating high-grade gliomas (HGGs) from low-grade gliomas (LGGs).

Methods PubMed and Embase databases were systematically searched for relevant studies of glioma grading assessed by MRS through 27 March 2015. Based on the data from eligible studies, pooled sensitivity, specificity, diagnostic odds ratio and areas under summary receiver operating characteristic curve (SROC) of different metabolite ratios were obtained.

Results Thirty articles comprising a total sample size of 1228 patients were included in our meta-analysis. Quantitative synthesis of studies showed that the pooled sensitivity/specificity of Cho/Cr, Cho/NAA and NAA/Cr ratios was 0.75/0.60, 0.80/0.76 and 0.71/0.70, respectively. The area under the curve (AUC) of the SROC was 0.83, 0.87 and 0.78, respectively.

Conclusions MRS demonstrated moderate diagnostic performance in distinguishing HGGs from LGGs using tumoural metabolite ratios including Cho/Cr, Cho/NAA and NAA/Cr. Although there was no significant difference in AUC between Cho/Cr and Cho/NAA groups, Cho/NAA ratio showed higher sensitivity and specificity than Cho/Cr ratio and NAA/Cr ratio. We suggest that MRS should combine other advanced imaging techniques to improve diagnostic accuracy in differentiating HGGs from LGGs.

Key points

- MRS has moderate diagnostic performance in distinguishing HGGs from LGGs.
- There is no significant difference in AUC between Cho/Cr and Cho/NAA ratios.
- Cho/NAA ratio is superior to NAA/Cr ratio.
- Cho/NAA ratio shows higher sensitivity and specificity than Cho/Cr and NAA/Cr ratios.
- MRS should combine other advanced imaging techniques to improve diagnostic accuracy.

Qun Wang, Hui Zhang and JiaShu Zhang contributed equally to this work.

✉ XiaoLei Chen
cx173@msn.com

✉ BaiNan Xu
bn_xu@yahoo.com

Qun Wang
wfwangqun@163.com

Hui Zhang
zhanghui198004@yahoo.com

JiaShu Zhang
shujiazhang@126.com

Chen Wu
bn_xu@yahoo.com; 13671007509@163.com

WeiJie Zhu
zhuweijie66@163.com

FangYe Li
leefangye@126.com

¹ Department of Neurosurgery, Chinese PLA General Hospital, 28 Fuxing Road, Haidian District, Beijing 100853, China

² Department of Neurosurgery, Air Force General Hospital of the Chinese PLA, 30 Fucheng Road, Haidian District, Beijing 100142, China

³ Department of Neurosurgery, General Hospital, Ji'nan Military Area Command, Ji'nan 250032, China

Keywords Magnetic resonance spectroscopy · Glioma · Differentiation · Systematic review · Meta-analysis

Abbreviations

AUC	Area under the curve
Cho	Choline
CI	Confidence intervals
Cr	Creatine
DOR	Diagnostic odds ratio
DTI	Diffusion tensor imaging
DWI	Diffusion-weighted imaging
FN	False negative
FP	False positive
HGGs	High-grade gliomas
I ²	Inconsistency index
Lac	Lactate
LGGs	Low-grade gliomas
LL	Lipids and lactate
LR+	Positive likelihood ratio
LR−	Negative likelihood ratio
LTE	Long echo time
MI	Myo-inositol
MRI	Magnetic resonance imaging
MRS	Magnetic resonance spectroscopy
MVS	Multi-voxel spectroscopy
NAA	<i>N</i> -acetyl-aspartate
nCho	Normalized choline
nCr	Normalized creatine
Pcr	Phosphocreatine
PET	Positron-emission tomography
QUADAS-2	Quality Assessment Tool for Diagnostic Accuracy Studies version 2
SEN	Sensitivity
SPE	Specificity
SPECT	Single photon mission computed tomography
SROC	Summary receiver-operating characteristic curve
STE	Short echo time
SVS	Single-voxel spectroscopy
TN	True negative
TP	True positive

Introduction

Gliomas are the most common primary neoplasm of the central nervous system, and the prognosis for this disease remains very poor [1]. In determining a treatment plan, tumour grade is a key consideration for minimizing the risk of unnecessary morbidity and mortality [2].

Given the limitations of conventional MRI in distinguishing low-grade gliomas (LGGs) from high-grade gliomas (HGGs) (accuracy between 55 % and 83 %), advanced multiparametric magnetic resonance (MR) techniques have been explored, including diffusion-weighted imaging (DWI), diffusion tensor imaging (DTI), proton MR spectroscopy (MRS) and perfusion imaging [3]. Because of its safety and non-invasive nature, MRS is of great advantage in patients with brain gliomas [4, 5]. MRS provides information about metabolic tissue composition, and advanced spectroscopic methods have been used to quantify markers of tumour metabolism (e.g. glucose), membrane turnover and proliferation (e.g. choline [Cho]), energy homeostasis (e.g. creatine [Cr]), intact glioneuronal structures (e.g. *N*-acetyl-aspartate [NAA]) and necrosis (e.g. lactate [Lac] or lipids) [6]. Results are usually expressed as ratios between cerebral metabolites rather than absolute concentrations [7].

Numerous studies have evaluated the diagnostic accuracy of ¹H-MR spectroscopy for distinguishing high- and low-grade gliomas. A systematic literature review [8] was performed approximately 10 years ago in order to provide evidence, but the interpretation was limited by the small number of studies and small sample sizes. In the current work, we performed a meta-analysis to measure the diagnostic performance of MRS in differentiating high- from low-grade gliomas.

Materials and methods

Search strategy

The PubMed and Embase databases were systematically searched to find relevant published articles (through 27 March 2015). We used the following keywords: (“magnetic resonance spectroscopy” or “MR spectroscopy” or “MRS”) AND (glioma). Additionally, the reference lists of all retrieved articles were checked for other eligible reports that were not identified in the initial search.

Inclusion and exclusion criteria

The inclusion criteria were as follows: (1) MRS was used to differentiate HGGs from LGGs in patients with no clinical history of previous surgery, chemotherapy or radiotherapy; (2) the diagnostic criteria of glioma grading were clearly stated, and the number of LGGs and HGGs could be obtained; (3) at least one individual metabolite ratio was used to evaluate the grading of glioma; (4) values of true positive (TP), false positive (FP), false negative (FN), true negative (TN), sensitivity (SEN), specificity (SPE), positive likelihood ratio (LR+) and negative likelihood ratio (LR−) could be accurately calculated from the data reported; (5) at least seven patients were

included; (6) pathology and/or clinical follow-up were used as the reference standard; (7) no data were overlapping; and (8) only English language full-text publications were included. The following were excluded: animal studies, abstracts, reviews, case report, letters, editorials, comments and conference proceedings.

Two authors (Q. Wang and H. Zhang) independently evaluated potentially relevant articles using the inclusion and exclusion criteria. If no agreement could be reached between these two authors, inconsistencies were discussed and resolved by a third author (B.N. Xu).

Data extraction and quality assessment

The screened articles were assessed independently by the same two authors (J.S. Zhang and X.L. Chen). For each included study, basal characteristics (authors, year of publication and country of origin), patient characteristics (number, mean age, sex, and grade of glioma) and technical aspects (imaging field strength, techniques of spectrum acquisition, device parameters, metabolite ratios, cut-off value, metabolite ratio mean value in different grades of glioma and reference standard) were noted. HGGs (grade III–IV gliomas) were considered positive; LGGs (grade I–II gliomas) were considered negative. The number of TP, FP, FN and TN results were calculated and recorded. The methodological quality of the studies was assessed using the Quality Assessment Tool for Diagnostic Accuracy Studies version 2 (QUADAS-2) [9]. Disagreements were resolved by consensus.

Statistical analysis

Standard methods recommended for meta-analysis diagnostic accuracy were used [10, 11]. First, heterogeneity was evaluated between studies in which this may have been caused by a threshold effect. A Spearman correlation coefficient was computed between the logit of SEN and the logit of (1–SPE) to assess the threshold effect, and the extent of heterogeneity was then assessed using the chi-square value test and the inconsistency index (I^2) of the diagnostic odds ratio (DOR). The existence of significant heterogeneity necessitated the use of a random-effects coefficient binary regression model when the test performance was summarized; otherwise, a fixed-effects coefficient binary regression model was used [12, 13].

The pooled SEN, SPE, LR+, LR– and DOR, with their 95 % confidence intervals (CIs), were calculated for each study. The summary receiver-operating characteristic curve (SROC), area under the curve (AUC) and Q^* index were calculated. AUC values of 51–70 %, 71–90 %, and >90 % indicated low, moderate and high diagnostic accuracy, respectively.

Subgroup analysis was performed when some homogeneous set of studies adopted similar design variables.

Subgroups were constructed only when more than three studies could be included. Tests of interaction were performed to assess differences between subgroups [14]. The above-mentioned statistical analyses were performed using Meta-DiSc statistical software version 1.4 [11].

Publication bias was assessed by Deeks' funnel plot. Formal testing for publication bias was conducted using a regression of the diagnostic log odds ratio against $ESS^{1/2}$ (effective sample size) and weighting according to the effective sample size, with $P < 0.10$ indicating significant asymmetry [15]. This statistical analysis was performed using Stata 12.0 software (StataCorp LP, College Station, TX, USA).

Results

Study selection and characteristics

The study selection process is described in Fig. 1. The systematic literature search included 30 articles [16–45] comprising a total sample of 1335 patients (1228 patients with MRS of appropriate quality) with radiologically suspected untreated glioma. The detailed characteristics of the included studies are listed in Table 1.

Among these studies, 25 were retrospective cohort studies, and only five studies were prospective. In 1228 patients with MRS of appropriate quality, there were 426 LGGs and 802 HGGs. The detailed grading of HGGs was available in all but two studies [17, 25]. Histological results obtained from either surgical biopsy and/or resection were the main reference standard in all studies. Both pathology and clinical follow-up combined with radiological follow-up were used as reference standard in three studies [17, 19, 21].

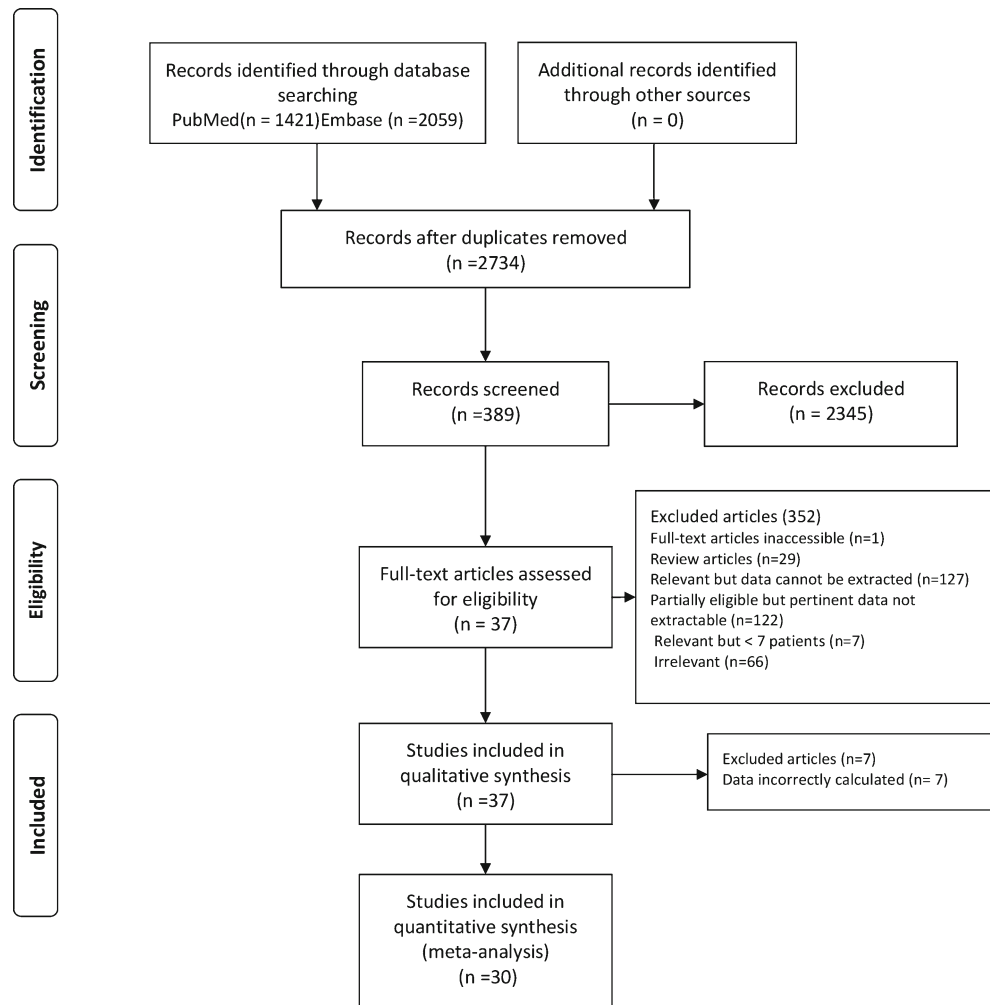
Most studies used a single metabolite ratio, while five articles used only combined diagnostic thresholds, i.e. Cho/Cr >1.2 and the presence of a lipid/lactate peak [19], either Cho/Cr ratio or Cho/NAA ratio >1.5 or the presence of lactate or lipids [24], Cho/Per-Cr and reduced NAA [41], Cho/Cr and/or LL/Cr [36], and Cho/Cr and NAA/Cho [43].

The risk of bias and concerns regarding the applicability of the studies are shown in Fig. 2. In most studies, the risk of bias was low or unclear. Three studies in which patients received a different reference standard were considered to have a high risk of bias.

Quantitative synthesis

Cho/Cr ratio

Overall, among 19 of the included studies, a total of 852 MRS examinations of good quality were performed for the detection of HGGs by calculating the Cho/Cr ratio [16–18, 20, 22, 23, 25, 27, 28, 30, 31, 33–35, 38–40, 42, 45]. The diagnostic

Fig. 1 Flow diagram of the study selection process

threshold of Cho/Cr ranged between 0.49 and 2.07. The Spearman correlation coefficient was 0.085 ($P=0.73$), which indicated that there was no obvious threshold effect in the estimates of accuracy. Significant heterogeneity was observed in the overall comparisons ($I^2=59\%$), and therefore the test performance was summarized using a random-effects coefficient binary regression model.

The pooled weighted values were determined as follows: SEN, 0.75 (95 % CI: 0.71, 0.79); SPE, 0.60 (95 % CI: 0.55, 0.66); LR+, 2.78 (95 % CI: 1.62, 4.76); LR-, 0.35 (95 % CI: 0.25, 0.49); and DOR, 8.53 (95 % CI: 4.39, 16.59). The forest plots from 19 studies are shown in Fig. 3A. The AUC under the SROC was 0.83 (Fig. 4A). A total of 313 MRS examinations among six studies were performed on 1.5-T scanners [27, 34, 39, 40, 42, 45]. A 3.0-T unit was used for 539 scans among 13 studies [16–18, 20, 22, 23, 25, 27, 28, 30, 31, 33–35, 38–40, 42, 45] that were included. There was no significant difference in AUC between the 1.5-T and 3.0-T subgroups ($P_{\text{interaction}}=0.77$).

Next, we performed subgroup analyses by spectrum acquisition technique (multi-voxel spectroscopy [MVS] and single-

voxel spectroscopy [SVS]) and echo time of the spectroscopic sequence (short echo time [STE] and long echo time [LTE]). There was no significant difference in the AUC between the MVS and SVS groups ($P_{\text{interaction}}=0.96$) or the STE and LTE groups ($P_{\text{interaction}}=0.90$). The results of the included studies and subgroup analyses of diagnostic accuracy variables are summarized in Table 2.

Cho/NAA ratio

A total of 603 MRS examinations were analyzed among 16 studies [26–33, 35, 37, 39–42, 44, 45] to detect HGGs from LGGs by calculating the Cho/NAA ratio. The diagnostic threshold of Cho/NAA ranged between 0.80 and 3.77. No threshold effect ($P=0.27$) or heterogeneity ($I^2=34\%$) was found among individual studies. The pooled SEN and SPE values were 0.80 (95 % CI: 0.76, 0.84) and 0.76 (95 % CI: 0.70, 0.82), respectively (Fig. 3B). The AUC under the SROC was 0.87 (Fig. 4B). The pooled SEN, SPE, LR+, LR-, DOR and AUC are summarized in Table 2. No significant

Table 1 Characteristics of studies included in the meta-analysis of MRS for the differential diagnosis of HGGs from LGGs

Author	Year	Country	Study design	No. of patients included	No. of patients with AQM	Age	M/F	Histology	HGG grading	Reference standard	Position of ROI	Imaging field strength	Voxel
Fudaba et al. [16]	2014	Japan	R	32	32	59.8(16-82)	13 M/19 F	LGG (9), HGG (23)	III (8), IV (15)	His: biopsy or resection	Intra	3.0-T	SVS (23) or MVS (9)
Dunet et al. [17]	2014	Switzerland	P	38	33	42(25-59)	26 M/12 F	LGG (15), HGG (18)	NA	His or follow	Intra	3.0-T	SVS
Caulo et al. [18]	2014	Italy	R	110	110	54(23-80)	66 M/44 F	LGG (33), HGG (77)	III (17), IV (60)	His: biopsy (97), resection (13)	Intra	3.0-T	MVS
Darveesh et al. [19]	2014	Egypt	R	36	20	17-76	17 M/19 F	LGG (7), HGG (13)	III (5), IV (8)	His or follow	Intra and Pen	1.5-T	SVS or MVS
Yoon et al. [20]	2014	Korea	R	60	60	50 (15-81)	35 M/25 F	LGG (12), HGG (48)	III (16), IV (32)	His: biopsy (20), resection (40)	Intra	3.0-T	SVS
Metwally et al. [21]	2014	Egypt	P	22	22	34.4 (15-63)	14 M/8 F	LGG (14), HGG (8)	III (2), IV (6)	His: (16), follow (6)	Intra	1.5-T	SVS or MVS
Sahin et al. [22]	2013	Turkey	R	20	20	44.3(28-64)	15 M/5 F	LGG (14), HGG (6)	III (6), IV (0)	His: biopsy (14), resection (6)	Intra	3.0-T	MVS
Roy et al. [23]	2013	India	R	56	56	44.3(14-69)	61 M/26 F	LGG (24), HGG (32)	III (12), IV (20)	His: biopsy or resection	Intra	3.0-T	MVS
Rao et al. [24]	2013	Australia	R	23	12	54(23-74)	11 M/12 F	LGG (3), HGG (9)	III (4), IV (5)	His: biopsy or resection	Intra	1.5-T	SVS or MVS
Chawalparit et al. [25]	2013	Thailand	P	43	40	45.4(12-75)	21 M/22 F	LGG (16), HGG (24)	NA	His: biopsy or resection	Intra	3.0-T	SVS or MVS
Aprile et al. [26]	2012	Italy	R	65	65	54.1(19-89)	42 M/23 F	LGG (22), HGG (43)	III (11), IV (32)	His: biopsy or resection	Intra	1.5-T	SVS (15) or MVS (50)
Shokry et al. [27]	2012	Egypt	R	15	15	42.2 (24-57)	8 M/7 F	LGG (5), HGG (10)	III (4), IV (6)	His: biopsy or resection	Intra	1.5-T	SVS
Liu et al. [28]	2012	China	R	32	32	44.8 (19-73)	20 M/13 F	LGG (10), HGG (22)	III (8), IV (14)	His: biopsy or resection	Intra	3.0-T	SVS
Zou et al. [29]	2011	China	P	30	30	46 (20-77)	42 M/23 F	LGG (12), HGG (18)	III (3), IV (15)	His: biopsy or resection	Intra	1.5-T	MVS
Zeng et al. [30]	2011	China	R	39	37	44.9(22-72)	23 M/16 F	LGG (12), HGG (25)	III (10), IV (15)	His: resection(37)	Intra	3.0-T	MVS
Withalm et al. [31]	2010	Austria	R	32	32	44(16-66)	16 M/16 F	LGG (13), HGG (19)	III (19), IV (0)	His: biopsy (5), resection (27)	Intra	3.0-T	MVS
Chernov et al. [32]	2008	Japan	P	71	49	39.4	48 M/23 F	LGG (18), HGG (31)	III (16), IV (17)	His: resection	Intra	1.5-T	SVS
Di Costanzo et al. [33]	2008	Italy	R	44	34	55.1±14	27 M/17 F	LGG (14), HGG (20)	III (5), IV (15)	His: biopsy or resection	Intra and Pen	3.0-T	MVS
Zonari et al. [34]	2007	Italy	R	105	105	44.7(15-77)	64 M/41 F	LGG (40), HGG (65)	III (45), IV (20)	His: biopsy or resection	Intra	1.5-T	SVS
Zhang et al. [35]	2007	China	R	41	41	45 (14-73)	15 M/26 F	LGG (16), HGG (25)	III (5), IV (20)	His: biopsy or resection	Intra	3.0-T	MVS
Kim et al. [36]	2006	Korea	R	35	35	47.3(23-71)	23 M/12 F	LGG (7), HGG (28)	III (12), IV (16)	His: biopsy (14), resection (21)	Intra	3.0-T	SVS
Stiedbauer et al. [37]	2006	Germany	R	26	26	37.5(18-63)	16 M/10 F	LGG (9), HGG (17)	III (17), IV (0)	His: biopsy (26)	Intra	1.5-T	MVS
Jeun et al. [38]	2005	Korea	R	12	12	50.3 (28-73)	4 M/8 F	LGG (3), HGG (9)	III (4), IV (5)	His: biopsy or resection	Intra	3.0-T	SVS
Magalhaes et al. [39]	2005	USA	R	16	16	43.2(22-68)	14 M/2 F	LGG (4), HGG (12)	III (3), IV (9)	His: biopsy (16)	Intra	1.5-T	SVS or MVS
Chen et al. [40]	2004	Taiwan	R	7	7	51(19-75)	2 M/5 F	LGG (5), HGG (2)	III (1), IV (1)	His: biopsy (7)	Intra	1.5-T	SVS
Fountas et al. [41]	2004	USA	R	71	71	46.2(34-76)	46 M/25 F	LGG (27), HGG (44)	III (18), IV (26)	His: biopsy (6), resection (65)	Intra	1.5-T	SVS
Law et al. [42]	2003	USA	R	160	160	43(4-82)	108 M/52 F	LGG (40), HGG (120)	III (73), IV (47)	His: biopsy (43), resection (117)	Intra	1.5-T	MVS

Table 1 (continued)

Author	Year	Country	Study design	No. of patients included	No. of patients with AQM	Age	M/F	Histology	HGG grading	Reference standard	Position of ROI	Imaging field strength	Voxel
Kumar et al. [43]	2003	India	R	60	29	30-65	35 M/25 F	LGG (15), HGG (14)	III (6), IV (8)	His: biopsy or resection	Intra	1.5-T	SYS or MVS
Yang et al. [44]	2002	Japan	R	17	17	46.8(14-67)	11 M/16 F	LGG (4), HGG (13)	III (5), IV (8)	His: biopsy (3), resection (14)	Intra	1.5-T	MVS
Furuya et al. [45]	1997	Japan	R	17	10	NA	NA	LGG (3), HGG (7)	III (4), IV (3)	His	Intra	1.5-T	MVS
Author	Head coil channel number	TE	Mean time for imaging (min)	Metabolite ratio	Cutoff	Mean value	TP	PP	FN	TN			
Fudaba et al. [16]	NA	LTE	6-9	Cho/Cr	>1.789	NA	21	2	2	7			
				Lac/Cr	>1.789	NA	17	0	6	9			
				NAA/Cho	>0.349	NA	16	2	7	7			
				NAA/Cr	>1.289	NA	7	0	16	9			
Dunet et al. [17]	NA	LTE	NA	Cho/Cr	>1.56	LGG: 2.1±1.3, HGG: 3.6±6.2	10	9	8	6			
Caulo et al. [18]	8-Channel	LTE	NA	Cho/Cr	>2.07	LGG: 1.372±0.76, HGG: 1.996±1.296	38	4	39	29			
Darweesh et al. [19]	Standard	LTE and STE	NA	Cho/Cr >1.2 and the presence of lipid/lactate peak		Intra: LGG: 1.85±0.494, Peri: LGG: 1.5±0.31, HGG: NA	13	0	0	7			
Yoon et al. [20]	8-Channel	STE	NA	Cho/Cr	>1.82	LGG: 1.54±0.31, HGG: 2.02±0.78	28	2	20	10			
Metwally et al. [21]	NA	LTE	40-50	MI/Cr	NA	LGG: 0.87±0.36, HGG: 3.57±4.29	31	1	17	11			
				Cho/Cr and LL/Cr			39	2	9	10			
				MI/Cr		LGG: 2±1.5, HGG: 0.39±0.15, 0.025±0.06	8	1	0	13			
Sahin et al. [22]	12-Channel	STE	NA	Cho/Cr	>1.3	LGG: 1.2±0.38, HGG: 1.2±0.38	6	4	0	10			
Roy et al. [23]	12-Channel	STE	26	Cho/Cr	>0.49	NA	24	9	8	15			
				Cho/T/ChoN	>0.57	NA	32	14	0	10			
				CreT/CreN	>0.41	NA	18	5	14	19			
Rao et al. [24]	Standard	LTE	NA	Cho/Cr ratio or Cho/NAA	>1.5	Cho/naa: LGG: 1.1±0.5, HGG: NA	9	1	0	2			
				ratio > 1.5 or by presence of lactate or lipids		Cho/cr: LGG: 1±0.1, HGG: NA							
Chawalparit et al. [25]	8-Channel	LTE or STE	NA	Cho/Cr	>1.7	LGG: 1.9 (1.3-10.5), HGG: 2.5 (1.5-5.5)	22	10	2	6			
Aprile et al. [26]	NA	LTE	NA	Cho/NAA	>1.84	LGG: 2.264±2.323, HGG: 3.7±2.8816	32	6	11	16			
Shokry et al. [27]	Quadrature	STE	40-54	Cho/NAA+Lac	>1.96	LGG: 1.6840±0.1658, HGG: 3.0170±1.8927	32	1	11	21			
				Cho/Cr	>1.83	LGG: 1.6640±0.1199, HGG: 3.3070±1.6050	19	0	0	5			
Lin et al. [28]		LTE	3	Cho/Cr	>2.01	LGG: 1.56±0.46, HGG: 3.06±1.89	16	1	3	9			
				Cho/NAA	>2.49	LGG: 1.68±0.89, HGG: 3.63±2.11	16	1	6	9			

Table 1 (continued)

Author	Year	Country	Study design	No. of patients included	No. of patients with AQM	Age	M/F	Histology	HGG grading	Reference standard	Position of ROI	Imaging field strength	Voxel
Zou et al. [29]	Standard	LTE	7	NAA/Cr	<0.97	LGG: 1.06±0.35, HGG: 1.68±0.89	17	3	5	7			
				NAA/Cho	<0.265	LGG: 0.51±0.22, HGG: 0.18±0.09	16	1	2	11			
				NAA/Cr	<0.66	LGG: 0.88±0.28, HGG: 0.49±0.14	16	1	2	11			
Zeng et al. [30]	NA	LTE	8	Cho/Cr	>2.04	LGG: 1.72±0.62, HGG: 2.94±1.83	21	2	4	10			
				Cho/NAA	>2.2	LGG: 1.97±1.10, HGG: 3.65±3.14	22	4	3	8			
				NAA/Cr	≤-0.72	LGG: 0.89±0.5, HGG: 0.72±0.35	19	4	6	8			
Widhalm et al. [31]	NA	LTE	7	Cho/Cr	>2.0	LGG: 1.8615±0.4753, HGG: 3.2053±1.8543	16	3	3	10			
				Cho/NAA	>1.9	LGG: 2.4197±1.8238, HGG: 5.4377±4.2126	18	4	1	9			
Chernov et al. [32]	Standard	LTE	NA	NAA/Cho	<0.6	LGG: 0.72 (0.56–1.03), HGG: 0.34 (0.16–0.44)	14	13	4	18			
Di Costanzo et al. [33]	Quadrature	LTE	NA	Cho/Cr	NA	LGG: 1.59±0.70, HGG: 2.85±1.18	11	3	9	11			
				Cho/NAA	NA	LGG: 1.89±1.11, HGG: 3.84±1.34	15	2	5	12			
				NAA/Cr	NA	LGG: 0.97±0.23, HGG: 0.84±0.52	15	6	5	8			
				Cho/Cr	NA	LGG: 1.51±0.64, HGG: 2.09±1.31	14	4	16	10			
				Cho/NAA	NA	LGG: 1.20±0.46, HGG: 2.92±1.38	19	1	11	13			
				NAA/Cr	NA	LGG: 1.26±0.44, HGG: 0.76±0.28	24	6	6	8			
Zonari et al. [34]	Standard	LTE	NA	NAA/Cr	<0.44	LGG: 0.69±0.41, HGG: 0.28±0.42	48	16	17	24			
				Cho/Cr	NA	LGG: 2.01±0.68, HGG: 2.47±1.28	57	39	8	1			
				Cho/NAA	>2.0	LGG: 1.559±0.419, HGG: 4.247±2.095	22	1	3	15			
Zhang et al. [35]	Standard	LTE	NA	Cho/Cr	>2.0	LGG: 1.793±0.386, HGG: 3.809±1.465	23	2	2	14			
Kim et al. [36]	Standard	STE	NA	Cho/Cr and/or LL/Cr	Cho/Cr >1.47LL/ Cr >1.63	LGG: 1.52±0.66, HGG: 2.17±0.79	25	3	3	4			
				Cho/Cr		LGG: 1.07±0.46, HGG: 6.17±8.33							
				Cho/Cr and/or LL/Cr	Cho/Cr >1.84LL/ Cr >0.59	LGG: 1.92±0.89, HGG: 3.56±3.10							
				Cho/Cr		LGG: 0.3±0.21, HGG: 2.56±4.17							
				LL/Cr			27	4	1	3			
		Combined											

Table 1 (continued)

Author	Year	Country	Study design	No. of patients included	No. of patients with AQM	Age	M/F	Histology	HGG grading	Reference standard	Position of ROI	Imaging field strength	Voxel
Stadlauer et al. [37]	Standard	LTE	13	Cho/NAA	>0.8	LGG: 0.40±0.16, HGG:0.81±0.46	17	0	0				
Jeun et al. [38]	Quadrature	STE		Cho/Cr	>0.91	LGG: 0.6±0.2685, HGG:2.1122±0.7174	9	0	0				
				NAA/Cr	>0.8	LGG: 0.4987±0.4145, HGG:0.65±0.3608	4	0	5				
				Lac/Cr	>1.65	LGG: 1.4833±0.1756, HGG:4.0133±2.4696	7	0	2				
Magalhaes et al. [39]		LTE	NA	Cho/Cr	>1.49	LGG: 1.5±0.4522, HGG:2.9167±3.0603	10	1	2				
				Cho/NAA	>2.61	LGG: 2.02±0.5158, HGG:5.3658±4.4058	8	0	4				
Chen et al. [40]	Standard	STE or LTE	NA	Cho/Cr	>1.97	LGG: 2.0976±1.3469, HGG:2.885±0.5586	2	1	0				
				Cho/NAA	>2.12	LGG: 1.7794±0.3679, HGG:3.6395±1.1575	2	0	0				
				NAA/Cr	>0.71	LGG: 0.876±0.2686, HGG:0.8±0.1131	2	3	0				
Fountas et al. [41]	Standard	LTE	18.1	Cho/Per-Cr and reduced NAA	NA	LGG: 2.15±0.26, HGG:NA	44	3	0				
Law et al. [42]	NA	LTE	NA	Cho/Cr	>1.56	LGG: 1.75±0.6, HGG:2.43±1.92	91	21	29				
				Cho/NAA	>1.60	LGG: 1.96±1.43, HGG:3.22±3.65	89	15	31				
Kumar et al. [43]	Standard	LTE	NA	Cho/Cr and NAA/Cho	NA		12	4	2				
Yang et al. [44]	Standard	LTE	12	Cho/NAA	>3.25	LGG: 4.89±2.9980, HGG:5.8954±2.6149	11	0	2				
				max NAA/Cr	>2.44	LGG: 1.84±1.1987, HGG:4.7285±2.2181	13	1	0				
				min NAA/Cr	<=0.44	LGG: 1.6475±1.6048, HGG:0.3977±0.0600	10	1	3				
Furuya et al. [45]	Standard	LTE	34	Cho/Cr	>0.98	LGG: 1.66±1.2831, HGG:2.5686±1.3145	7	1	0				
				Cho/NAA	>0.93	LGG: 1.1533±0.5314, HGG:2.4486±1.188	7	1	0				
				NAA/Cr	<1.03	LGG: 1.3133±0.4053, HGG:1.1871±0.6963	4	0	3				

AQM appropriate quality of MRS; His histology; F female; HGG high-grade glioma; Intra intratumoural; LGG low-grade glioma; M male; Max maximum; Min minimum; NA not available; P prospective; Peri peritumoural; R retrospective; Standard standard head coil; Quadrature quadrature head coil

Fig. 2 Methodological quality analysis of the 30 eligible studies using QUADAS-2 tool

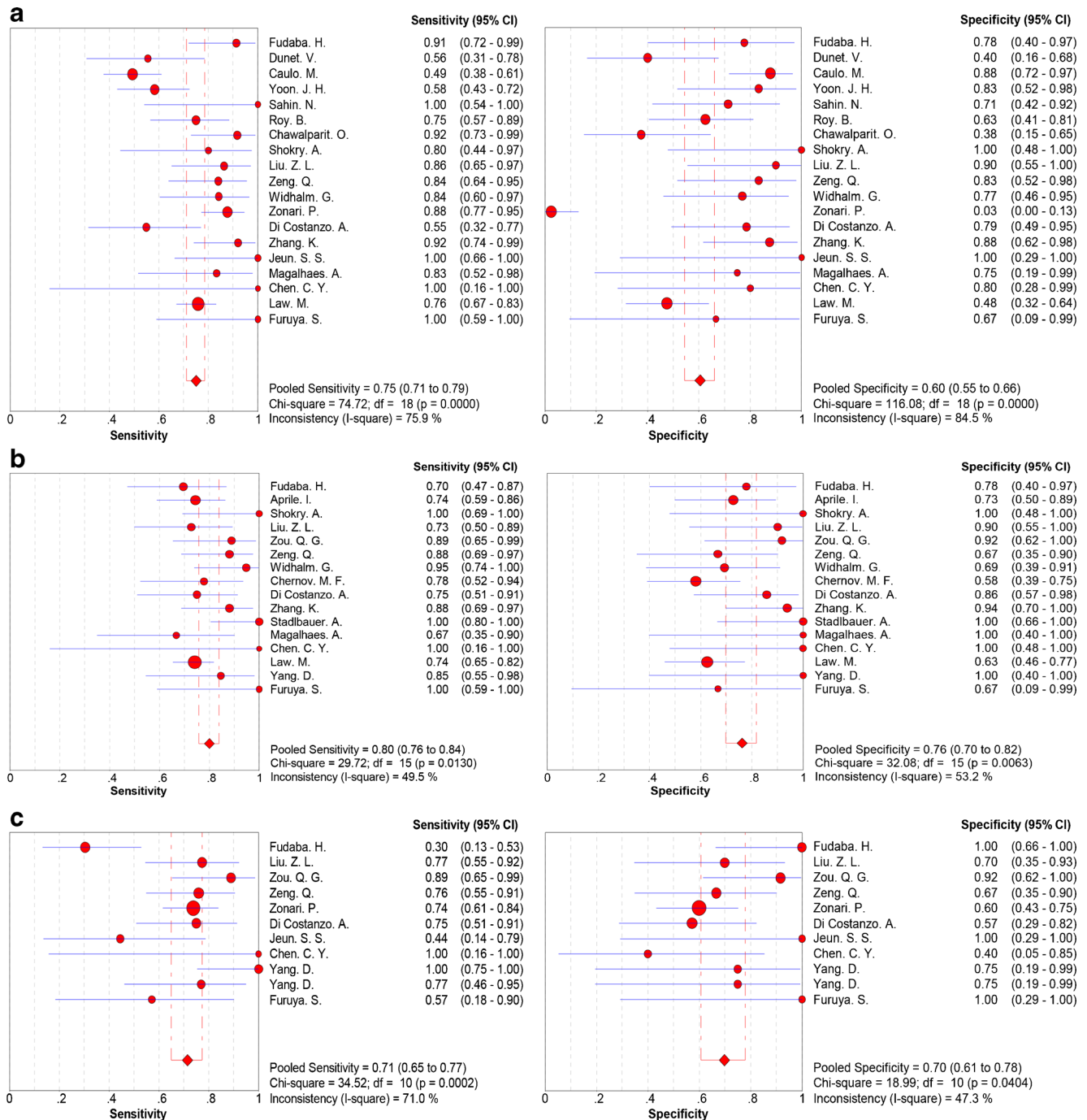
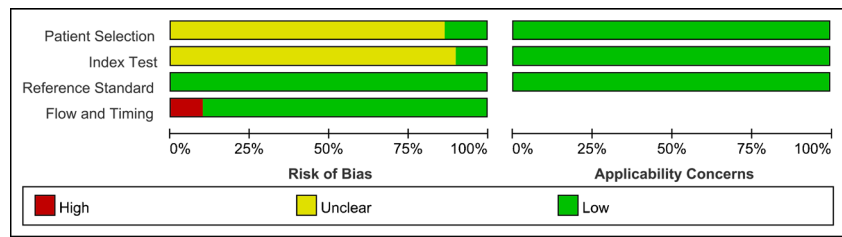


Fig. 3 Forest plot showing the sensitivity and specificity of different metabolite ratios for the differentiation of HGGs from LGGs. (A) Cho/Cr ratio; (B) Cho/NAA ratio; (C) NAA/Cr ratio

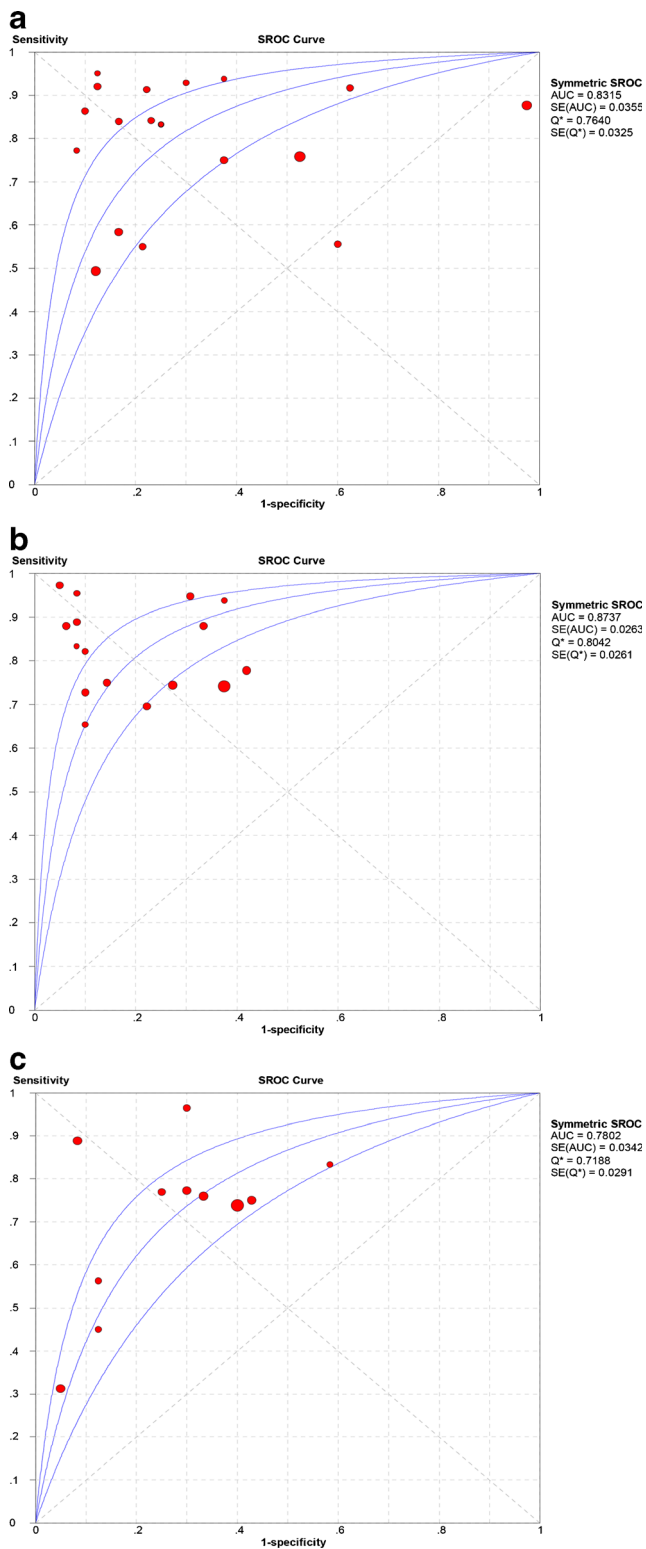


Fig. 4 Summary receiver-operating characteristic curve (SROC). (A) Cho/Cr ratio; (B) Cho/NAA ratio; (C) NAA/Cr ratio. AUC area under the curve

difference in AUC was detected between the 1.5-T and 3.0-T subgroups ($P_{\text{interaction}}=0.76$) or the MVS and SVS subgroups ($P_{\text{interaction}}=0.35$).

NAA/Cr ratio

Ten studies [16, 28–30, 33, 34, 38, 40, 44, 45] including 333 MRS examinations were conducted in which HGGs were detected by calculating the NAA/Cr ratio. The diagnostic threshold of NAA/Cr ranged between 0.44 and 2.44. Here there was also no threshold effect ($P=0.35$) or heterogeneity ($I^2=0.0\%$) found among individual studies. The pooled SEN and SPE were 0.71 (95 % CI: 0.65, 0.77) and 0.70 (95 % CI: 0.61, 0.78), respectively (Fig. 3C). The AUC under the SROC was 0.78 (Fig. 4C). No significant difference in AUC was detected between the 1.5-T and 3.0-T subgroups ($P_{\text{interaction}}=0.39$) or the MVS and SVS subgroups ($P_{\text{interaction}}=0.31$).

LL/Cr

Only two studies [20, 36] had been performed in which HGGs were detected by calculating the ratio of lipids and lactate (LL)/Cr. Quantitative synthesis of studies measuring other metabolite ratios was impossible because of limited data. Finally, we compared the AUCs among the three groups, which revealed significant differences in AUC between the Cho/NAA and NAA/Cr groups ($P_{\text{interaction}}=0.03$).

Sensitivity analysis

Among the 19 included studies in which HGGs were detected by calculating the Cho/Cr ratio, the DOR values were greater than 1.0 in all but two studies [17, 34], which were then excluded from the sensitivity analysis. The corresponding pooled SEN, SPE, LR+, LR– and DOR were 0.74 (95 % CI: 0.70, 0.78), 0.72 (95 % CI: 0.65, 0.77), 2.8 (95 % CI: 2.02, 3.88), 0.31 (95 % CI: 0.22, 0.43) and 10.92 (95 % CI: 6.26, 19.06), respectively. The AUC under the SROC was 0.84, which was not materially different from the overall AUC (0.83), indicating that our results were statistically robust.

Heterogeneity analysis and publication bias

Significant heterogeneity was present in the pooled analysis in the Cho/Cr group that could not be explained by threshold effect. Meta-regression analysis showed that factors including year of publication, country, study design, compact surface, voxel, and echo time did not contribute to heterogeneity. There was no significant heterogeneity in the pooled analysis in the Cho/NAA and NAA/Cr groups.

The Deeks’ funnel plot asymmetry test for the overall analysis in the Cho/Cr, Cho/NAA and NAA/Cr groups showed that publication bias may have existed in Cho/Cr and Cho/NAA groups ($P=0.01$ and 0.02, respectively) (Fig. 5A, B), while the NAA/Cr group showed no significant publication bias ($P=0.31$) (Fig. 5C).

Table 2 Subgroup analyses of diagnostic accuracy variables

Category	Study (n)	Threshold effects (P value)	I ² (%)	SEN (95 % CI)	SPE (95 % CI)	LR+ (95 % CI)	LR- (95 % CI)	DOR (95 % CI)	AUC (SE)
Cho/Cr									
Overall	19	0.729	59.4	0.75 [0.71, 0.79]	0.60 [0.55, 0.66]	2.78 [1.62, 4.76]	0.35 [0.25, 0.49]	8.53 [4.39, 16.59]	0.8315 (0.0355)
1.5-T	6	0.572	61.0	0.81 [0.75, 0.86]	0.35 [0.26, 0.45]	1.91 [0.89, 4.09]	0.40 [0.19, 0.87]	4.73 [1.03, 21.79]	0.8149 (0.0508)
3.0-T	13	0.971	53.2	0.71 [0.66, 0.76]	0.73 [0.66, 0.79]	2.82 [1.85, 4.29]	0.32 [0.21, 0.49]	10.62 [5.15, 21.90]	0.8338 (0.0386)
MVS	9	0.635	49.4	0.72 [0.66, 0.76]	0.71 [0.64, 0.78]	2.73 [1.82, 4.09]	0.36 [0.24, 0.54]	9.03 [4.35, 18.75]	0.8202 (0.0384)
SVS	7	0.879	74.1	0.76 [0.69, 0.83]	0.42 [0.32, 0.53]	2.86 [0.82, 9.97]	0.44 [0.21, 0.92]	6.41 [1.13, 36.36]	0.8166 (0.0777)
STE	5	0.624	2.4	0.71 [0.62, 0.80]	0.74 [0.61, 0.85]	2.94 [1.86, 4.65]	0.34 [0.23, 0.49]	9.00 [4.08, 19.89]	0.8229 (0.0534)
LTE	12	0.863	72.4	0.75 [0.70, 0.79]	0.58 [0.51, 0.65]	2.76 [1.31, 5.82]	0.36 [0.23, 0.55]	7.87 [3.13, 19.81]	0.8308 (0.0493)
Cho/NAA									
Overall	16	0.270	34.2	0.80 [0.76, 0.84]	0.76 [0.70, 0.82]	3.32 [2.59, 4.25]	0.26 [0.21, 0.32]	11.95 [8.10, 17.63]	0.8737 (0.0263)
1.5-T	10	0.075	43.0	0.79 [0.74, 0.84]	0.73 [0.56, 0.81]	2.93 [2.20, 3.91]	0.28 [0.21, 0.37]	9.35 [5.93, 14.75]	0.8740 (0.0394)
3.0-T	6	0.577	0.0	0.81 [0.74, 0.88]	0.81 [0.70, 0.89]	4.31 [2.68, 6.92]	0.22 [0.15, 0.32]	21.62 [10.10, 46.27]	0.8891 (0.0296)
LTE	14	0.695	34.9	0.79 [0.75, 0.83]	0.75 [0.68, 0.81]	3.20 [2.49, 4.10]	0.27 [0.21, 0.33]	11.30 [7.62, 16.76]	0.8649 (0.0275)
SVS	4	0.262	35.9	0.81 [0.67, 0.90]	0.73 [0.58, 0.84]	3.23 [1.90, 5.50]	0.27 [0.15, 0.47]	11.28 [4.34, 29.36]	0.8545 (0.0509)
MVS	9	0.389	54.4	0.82 [0.77, 0.88]	0.77 [0.69, 0.85]	3.50 [2.14, 5.75]	0.19 [0.11, 0.33]	26.92 [9.50, 76.30]	0.9118 (0.0334)
NAA/Cr									
Overall	11	0.353	0.0	0.71 [0.65, 0.77]	0.70 [0.61, 0.78]	2.4 [1.81, 3.19]	0.40 [0.32, 0.51]	6.67 [4.10, 10.85]	0.7802 (0.0342)
1.5-T	6	0.957	29.7	0.79 [0.70, 0.86]	0.68 [0.55, 0.78]	2.43 [1.70, 3.49]	0.33 [0.22, 0.47]	7.19 [3.84, 13.46]	0.8401 (0.0663)
3.0-T	5	0.285	0.0	0.63 [0.52, 0.72]	0.73 [0.58, 0.85]	2.35 [1.48, 3.72]	0.50 [0.37, 0.66]	5.98 [2.75, 12.99]	0.7682 (0.0517)
LTE	9	0.831	0.0	0.72 [0.66, 0.78]	0.70 [0.61, 0.79]	2.43 [1.81, 3.27]	0.39 [0.31, 0.50]	6.81 [4.14, 11.21]	0.7832 (0.0355)
SVS	4	0.200	0.0	0.72 [0.63, 0.81]	0.62 [0.48, 0.74]	1.97 [1.38, 2.80]	0.43 [0.30, 0.63]	4.79 [2.47, 9.26]	0.7506 (0.0586)
MVS	6	0.704	0.0	0.80 [0.71, 0.88]	0.73 [0.59, 0.85]	2.89 [1.82, 4.59]	0.28 [0.19, 0.44]	9.73 [4.58, 20.69]	0.8340 (0.0586)

SE standard error

Discussion

Metabolic ratios of MRS have been frequently used to differentiate glioma grade among numerous studies. In an earlier article [8], the sensitivity and specificity of MRS was reviewed only in terms of differentiating high- from low-grade tumours. A recently published meta-analysis [46] concluded that MRS demonstrated moderate sensitivity and specificity for discriminating brain tumours (pooled estimates of 80.58 % and 78.46 %, respectively). The chief problem in this meta-analysis is that the authors combined all related articles without identifying gliomas from brain tumours or differentiating metabolite ratios used in each study, which would inevitably increase heterogeneity and render the conclusion unreliable [7]. We performed the present systematic review and meta-analyses based on accurate calculations of the relevant data.

Cho/Cr ratio

According to the quantitative synthesis, the AUC of the SROC curve was 0.83, suggesting a moderate level of overall accuracy. The DOR is a single indicator of test accuracy that combines the SEN and SPE data into a single number [47]. In this meta-analysis, the pooled DOR for diagnostic accuracy of glioma grading using

the Cho/Cr ratio was 8.53, indicating that this ratio may be helpful in the diagnosis of glioma grade. As the likelihood ratios are considered clinically more meaningful than SROC curve and DOR, both LR+ and LR- were also calculated to assess diagnostic accuracy. An LR+ of 2.78 suggests that HGG patients have about threefold higher odds of a positive test (> cut-off value) than LGG patients. On the other hand, the LR- was 0.35, suggesting that with a low cut-off value for the Cho/Cr ratio, the probability of HGG for this patient would be 35 %, which is not low enough to rule out HGG.

The results of subgroup analysis showed no significant difference in diagnostic accuracy between 3.0-T and 1.5-T MRS. However, in light of the limited data, further verification of these results is needed. The diagnostic performance of both the MVS and SVS techniques in distinguishing HGGs from LGGs was mediocre, and showed no statistical difference in either LTE or STE subgroup.

Significant heterogeneity was observed in the overall comparisons that could not be explained by threshold effect. Despite performing meta-regression analysis, we were unable to find the source of the heterogeneity. There may be publication bias with regard to the Cho/Cr ratio (Fig. 5A), as the results of Deeks' funnel plot asymmetry test ($P=0.01$) indicated that only small studies with high accuracy had been reported, while small studies with lower accuracy likely had not.

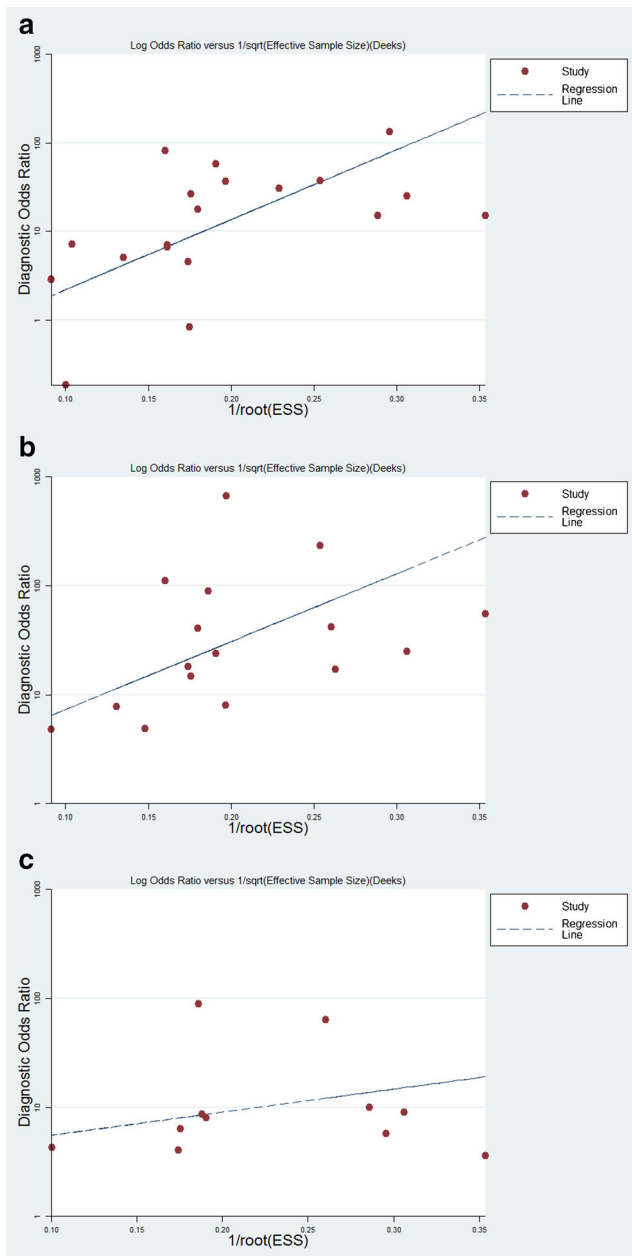


Fig. 5 Funnel plot of publication bias. (A) Cho/Cr ratio; (B) Cho/NAA ratio; (C) NAA/Cr ratio

Cho/NAA ratio

For the Cho/NAA ratio, the AUC (0.87) indicated a moderate level of overall accuracy. The pooled DOR of diagnostic accuracy for HGG detection by the Cho/NAA ratio was 11.95, indicating that the ratio may be helpful in the diagnosis of HGGs. No statistically significant difference in diagnostic accuracy was detected between the 1.5-T and 3.0-T or MVS and SVS subgroups. Because of the limited STE study data, we were unable to compare the diagnostic performance of the Cho/NAA ratio between LTE and STE. No heterogeneity was present in the overall comparisons, but publication bias

may exist, due to the small study effects (the tendency for the small studies in a meta-analysis to show high accuracy).

NAA/Cr ratio

With regard to the NAA/Cr ratio, the AUC (0.78) indicated a moderate level of overall accuracy. The summary DOR of the diagnostic accuracy of the Cho/NAA ratio in detecting HGGs was 6.67, indicating that the ratio may be helpful in diagnosing HGGs. No statistically significant difference in diagnostic accuracy was detected between the 1.5-T and 3.0-T or MVS and SVS subgroups. Heterogeneity and publication bias was not present in the overall comparisons, indicating that the results for the NAA/Cr ratio in our meta-analysis were statistically robust.

Overall comparisons between different metabolite ratios

Several studies have strongly recommended the use of the Cho/NAA ratio rather than the Cho/Cr ratio for differentiating HGGs from LGGs [44, 48–50], and one study noted no significant differences in the tumoural Cho/Cr ratio between LGGs and HGGs [48]. Cho/Cr is the ratio most frequently used, as mentioned in an overview of MRS [51] and supported by other authors [52, 53]. This ratio has also demonstrated reasonably low overall error during image processing [54]. Another reason for its use is that creatine concentration is known to be relatively stable during the formation of the anaplastic foci, in contrast to Cho concentration, which increases progressively [4]. However, this is a controversial issue, and one study [55] showed that creatine can change during the course of glioma development, and that creatine concentration can even carry prognostic information.

It is noteworthy that our meta-analysis showed no significant difference in AUC between the Cho/Cr and Cho/NAA groups ($P_{\text{interaction}} > 0.05$) or between the Cho/Cr and NAA/Cr groups, but that there was a significant difference in AUC between the Cho/NAA and NAA/Cr groups ($P_{\text{interaction}} < 0.05$), thus demonstrating that the Cho/NAA ratio has higher diagnostic accuracy than the NAA/Cr ratio in distinguishing HGGs from LGGs.

Based on the overall study results, the sensitivity and specificity of glioma grade diagnosis was higher for the Cho/NAA ratio (SE=0.80, SP=0.76) than the Cho/Cr ratio (SE=0.75, SP=0.60) or NAA/Cr ratio (SE=0.71, SP=0.70). Taking this diagnostic performance into consideration, the Cho/NAA ratio may be a superior index for distinguishing HGGs from LGGs. However, given the limited data, further study is needed to confirm the efficacy of the Cho/NAA ratio.

Limitations

Although the present meta-analysis revealed moderate overall diagnostic accuracy for MRS in distinguishing HGGs from LGGs, some design limitations should be taken into consideration when interpreting our results.

First, most of the included articles focused on the diagnostic efficiency of a single metabolite ratio. The standards combined different metabolites with metabolite ratios in distinguishing HGGs from LGGs, but these were not well established. Thus it was difficult to perform an accurate statistical analysis, as it was not known whether combined standards could improve diagnostic accuracy. In addition, the focus of the analysis was the superior metabolite ratios of tumour tissue, and comparisons between tumour tissue and healthy tissue were lacking, which may have led to lower specificity.

Second, as mentioned above, several innovative and advanced multiparametric magnetic resonance techniques, including DWI, DTI, and MR perfusion and multimodal imaging including PET/SPECT, also help to distinguish HGGs from LGGs. Though it is controversial which imaging technique is superior, most authors concluded that combined techniques would improve diagnostic accuracy [17, 22, 29, 34, 54].

Third, heterogeneity was found among the Cho/Cr ratio groups, and factors such as sample size, patient age and glioma grade may have also contributed to heterogeneity. Although heterogeneity was not present in the other two groups, there was considerable variation in study design, such as different types of coils, MRI devices and diverse methods of determining cut-off values. Fourth, there may have been publication bias regarding the Cho/Cr and Cho/NAA groups. Our meta-analysis was based only on published studies, which tend to report high accuracy; studies with lower accuracy are often rejected or not even submitted. In addition, this review was restricted to full-text articles published in English, thus omitting eligible studies that were unpublished or reported in other languages, which also likely resulted in bias.

Fifth, different spectroscopic patterns of glial tumour grades were not reflected. High-grade tumours in these studies represented grade III and IV cases grouped together, whereas a major diagnostic challenge sometimes is differentiating grade II from grade III and grade III from grade IV. Dividing the subgroups would have changed the cut-off threshold. Finally, the studies with small sample sizes would be greatly affected by adding 0.5 to each cell of the study to correct for zero entries in order to avoid potential problems in odds calculations for studies with sensitivity or specificity of 100 %.

In conclusion, this meta-analysis provides evidence that MRS has moderate diagnostic performance in distinguishing HGGs from LGGs using tumoural metabolite ratios. The Cho/NAA ratio is superior to the NAA/Cr ratio in differentiating between HGGs and LGGs. We suggest that MRS should be

combined with other advanced imaging techniques in order to improve diagnostic accuracy.

Acknowledgments The scientific guarantor of this publication is Hui Zhang, PHD. The authors of this manuscript declare no relationships with any companies whose products or services may be related to the subject matter of the article. The authors state that this work has not received any funding. One of the authors (Hui Zhang) has significant statistical expertise. Neither institutional review board approval nor written informed consent were required, because of the nature of our study, which was a systemic review and meta-analysis. Methodology: Meta-analysis, performed at one institution.

References

- Inoue T, Ogasawara K, Beppu T, Ogawa A, Kabasawa H (2005) Diffusion tensor imaging for preoperative evaluation of tumor grade in gliomas. *Clin Neurol Neurosurg* 107:174–180
- Lu H, Pollack E, Young R et al (2008) Predicting grade of cerebral glioma using vascular-space occupancy MR imaging. *AJNR Am J Neuroradiol* 29:373–378
- Chung C, Metser U, Menard C (2015) Advances in magnetic resonance imaging and positron emission tomography imaging for grading and molecular characterization of glioma. *Semin Radiat Oncol* 25:164–171
- Bulik M, Jancalek R, Vanicek J, Skoch A, Mechl M (2013) Potential of MR spectroscopy for assessment of glioma grading. *Clin Neurol Neurosurg* 115:146–153
- Herminghaus S, Dierks T, Pilatus U et al (2003) Determination of histopathological tumor grade in neuroepithelial brain tumors by using spectral pattern analysis of in vivo spectroscopic data. *J Neurosurg* 98:74–81
- Dhermain FG, Hau P, Lanfermann H, Jacobs AH, van den Bent MJ (2010) Advanced MRI and PET imaging for assessment of treatment response in patients with gliomas. *Lancet Neurol* 9:906–920
- Zhang H, Ma L, Wang Q, Zheng X, Wu C, Xu BN (2014) Role of magnetic resonance spectroscopy for the differentiation of recurrent glioma from radiation necrosis: a systematic review and meta-analysis. *Eur J Radiol* 83:2181–2189
- Hollingsworth W, Medina LS, Lenkinski RE et al (2006) A systematic literature review of magnetic resonance spectroscopy for the characterization of brain tumors. *AJNR Am J Neuroradiol* 27:1404–1411
- Whiting PF, Rutjes AW, Westwood ME et al (2011) QUADAS-2: a revised tool for the quality assessment of diagnostic accuracy studies. *Ann Intern Med* 155:529–536
- Deville WL, Buntinx F, Bouter LM et al (2002) Conducting systematic reviews of diagnostic studies: didactic guidelines. *BMC Med Res Methodol* 2:9
- Zamora J, Abaira V, Muriel A, Khan K, Coomarasamy A (2006) Meta-DiSc: a software for meta-analysis of test accuracy data. *BMC Med Res Methodol* 6:31
- Higgins JP, Thompson SG, Deeks JJ, Altman DG (2003) Measuring inconsistency in meta-analyses. *BMJ* 327:557–560
- Leeflang MM, Deeks JJ, Gatsonis C, Bossuyt PM (2008) Systematic reviews of diagnostic test accuracy. *Ann Intern Med* 149:889–897
- Altman DG, Bland JM (2003) Interaction revisited: the difference between two estimates. *BMJ* 326:219
- Deeks JJ, Macaskill P, Irwig L (2005) The performance of tests of publication bias and other sample size effects in systematic reviews of diagnostic test accuracy was assessed. *J Clin Epidemiol* 58:882–893

16. Fudaba H, Shimomura T, Abe T et al (2014) Comparison of multiple parameters obtained on 3T pulsed arterial spin-labeling, diffusion tensor imaging, and MRS and the Ki-67 labeling index in evaluating glioma grading. *AJNR Am J Neuroradiol* 35:2091–2098
17. Dunet V, Maeder P, Nicod-Lalonde M et al (2014) Combination of MRI and dynamic FET PET for initial glioma grading. *Nuklearmedizin* 53:155–161
18. Caulo M, Panara V, Tortora D et al (2014) Data-driven grading of brain gliomas: a multiparametric MR imaging study. *Radiology* 272:494–503
19. Darweesh AMN, Badawy ME, Hamesa M, Saber N (2014) Magnetic resonance spectroscopy and diffusion imaging in the evaluation of neoplastic brain lesions. *Egypt J Radiol Nucl Med* 45:485–493
20. Yoon JH, Kim JH, Kang WJ et al (2014) Grading of cerebral glioma with multiparametric MR imaging and 18F-FDG-PET: concordance and accuracy. *Eur Radiol* 24:380–389
21. Metwally LIA, El-Din SE, Abdelaziz O, Hamdy IM, Elsamman AK, Abdelalim AM (2014) Predicting grade of cerebral gliomas using Myo-inositol/Creatine ratio. *Egypt J Radiol Nucl Med* 45:211–217
22. Sahin N, Melhem ER, Wang S et al (2013) Advanced MR imaging techniques in the evaluation of nonenhancing gliomas: perfusion-weighted imaging compared with proton magnetic resonance spectroscopy and tumor grade. *Neuroradiol J* 26:531–541
23. Roy B, Gupta RK, Maudsley AA et al (2013) Utility of multiparametric 3-T MRI for glioma characterization. *Neuroradiology* 55:603–613
24. Rao PJ, Jyoti R, Mews PJ, Desmond P, Khurana VG (2013) Preoperative magnetic resonance spectroscopy improves diagnostic accuracy in a series of neurosurgical dilemmas. *Br J Neurosurg* 27:646–653
25. Chawalparit O, Sangruchi T, Witthiwej T et al (2013) Diagnostic performance of advanced MRI in differentiating high-grade from low-grade gliomas in a setting of routine service. *J Med Assoc Thai* 96:1365–1373
26. Aprile I, Tomi C, Fiaschini P, Muti M (2012) High-Grade Cerebral Glioma Characterization: Usefulness of MR Spectroscopy and Perfusion Imaging Associated Evaluation. *Neuroradiol J* 25:57–66
27. Shokry A (2012) MRS of brain tumors: diagrammatic representations and diagnostic approach. *Egypt J Radiol Nucl Med* 43:603–612
28. Liu ZL, Zhou Q, Zeng QS, Li CF, Zhang K (2012) Noninvasive evaluation of cerebral glioma grade by using diffusion-weighted imaging-guided single-voxel proton magnetic resonance spectroscopy. *J Int Med Res* 40:76–84
29. Zou QG, Xu HB, Liu F, Guo W, Kong XC, Wu Y (2011) In the assessment of supratentorial glioma grade: the combined role of multivoxel proton MR spectroscopy and diffusion tensor imaging. *Clin Radiol* 66:953–960
30. Zeng Q, Liu H, Zhang K, Li C, Zhou G (2011) Noninvasive evaluation of cerebral glioma grade by using multivoxel 3D proton MR spectroscopy. *Magn Reson Imaging* 29:25–31
31. Widhalm G, Krssak M, Minchev G et al (2011) Value of ¹H-magnetic resonance spectroscopy chemical shift imaging for detection of anaplastic foci in diffusely infiltrating gliomas with non-significant contrast-enhancement. *J Neurol Neurosurg Psychiatry* 82:512–520
32. Chernov MF, Ono Y, Muragaki Y et al (2008) Differentiation of high-grade and low-grade gliomas using pattern analysis of long-echo single-voxel proton magnetic resonance spectroscopy ((1)H-MRS). *Neuroradiol J* 21:338–349
33. Di CA, Scarabino T, Trojsi F et al (2008) Proton MR spectroscopy of cerebral gliomas at 3 T: spatial heterogeneity, and tumour grade and extent. *Eur Radiol* 18:1727–1735
34. Zonari P, Baraldi P, Crisi G (2007) Multimodal MRI in the characterization of glial neoplasms: the combined role of single-voxel MR spectroscopy, diffusion imaging and echo-planar perfusion imaging. *Neuroradiology* 49:795–803
35. Zhang K, Li C, Liu Y et al (2007) Evaluation of invasiveness of astrocytoma using ¹H-magnetic resonance spectroscopy: correlation with expression of matrix metalloproteinase-2. *Neuroradiology* 49:913–919
36. Kim JH, Chang KH, Na DG et al (2006) 3T ¹H-MR spectroscopy in grading of cerebral gliomas: comparison of short and intermediate echo time sequences. *AJNR Am J Neuroradiol* 27:1412–1418
37. Stadlbauer A, Gruber S, Nimsky C et al (2006) Preoperative grading of gliomas by using metabolite quantification with high-spatial-resolution proton MR spectroscopic imaging. *Radiology* 238:958–969
38. Jeun SS, Kim MC, Kim BS et al (2005) Assessment of malignancy in gliomas by 3T ¹H MR spectroscopy. *Clin Imaging* 29:10–15
39. Magalhaes A, Godfrey W, Shen Y, Hu J, Smith W (2005) Proton magnetic resonance spectroscopy of brain tumors correlated with pathology. *Acad Radiol* 12:51–57
40. Chen CY, Ling JF, Chan WP, Fang CL (2004) Proton magnetic resonance spectroscopy-guided biopsy for cerebral glial tumors. *J Formos Med Assoc* 103:448–458
41. Fountas KN, Kapsalaki EZ, Vogel RL, Fezoulidis I, Robinson JS, Gotsis ED (2004) Noninvasive histologic grading of solid astrocytomas using proton magnetic resonance spectroscopy. *Stereotact Funct Neurosurg* 82:90–97
42. Law M, Yang S, Wang H et al (2003) Glioma grading: sensitivity, specificity, and predictive values of perfusion MR imaging and proton MR spectroscopic imaging compared with conventional MR imaging. *AJNR Am J Neuroradiol* 24:1989–1998
43. Kumar A, Kaushik S, Tripathi RP, Kaur P, Khushu S (2003) Role of in vivo proton MR spectroscopy in the evaluation of adult brain lesions: our preliminary experience. *Neurol India* 51:474–478
44. Yang D, Korogi Y, Sugahara T et al (2002) Cerebral gliomas: prospective comparison of multivoxel 2D chemical-shift imaging proton MR spectroscopy, echo-planar perfusion and diffusion-weighted MRI. *Neuroradiology* 44:656–666
45. Furuya S, Naruse S, Ide M et al (1997) Evaluation of metabolic heterogeneity in brain tumors using ¹H-chemical shift imaging method. *NMR Biomed* 10:25–30
46. Wang W, Hu Y, Lu P et al (2014) Evaluation of the diagnostic performance of magnetic resonance spectroscopy in brain tumors: a systematic review and meta-analysis. *PLoS One* 9, e112577
47. Glas AS, Lijmer JG, Prins MH, Bossel GJ, Bossuyt PM (2003) The diagnostic odds ratio: a single indicator of test performance. *J Clin Epidemiol* 56:1129–1135
48. Server A, Kulle B, Gadmar OB, Josefsen R, Kumar T, Nakstad PH (2011) Measurements of diagnostic examination performance using quantitative apparent diffusion coefficient and proton MR spectroscopic imaging in the preoperative evaluation of tumor grade in cerebral gliomas. *Eur J Radiol* 80:462–470
49. Chen J, Huang SL, Li T, Chen XL (2006) In vivo research in astrocytoma cell proliferation with ¹H-magnetic resonance spectroscopy: correlation with histopathology and immunohistochemistry. *Neuroradiology* 48:312–318
50. Moller-Hartmann W, Herminghaus S, Krings T et al (2002) Clinical application of proton magnetic resonance spectroscopy in the diagnosis of intracranial mass lesions. *Neuroradiology* 44:371–381
51. Bertholdo D, Watcharakom A, Castillo M (2013) Brain proton magnetic resonance spectroscopy: introduction and overview. *Neuroimaging Clin N Am* 23:359–380
52. Howe FA, Barton SJ, Cudlip SA et al (2003) Metabolic profiles of human brain tumors using quantitative in vivo ¹H magnetic resonance spectroscopy. *Magn Reson Med* 49:223–232
53. Pamir MN, Ozduman K, Yildiz E, Sav A, Dincer A (2013) Intraoperative magnetic resonance spectroscopy for identification of residual tumor during low-grade glioma surgery: clinical article. *J Neurosurg* 118:1191–1198

54. Bradac O, Vrana J, Jiru F et al (2014) Recognition of anaplastic foci within low-grade gliomas using MR spectroscopy. *Br J Neurosurg* 28:631–636
55. Hattingen E, Raab P, Franz K et al (2008) Prognostic value of choline and creatine in WHO grade II gliomas. *Neuroradiology* 50:759–767